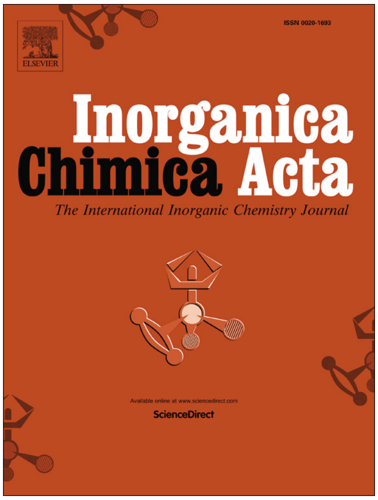

Research paper

Synthesis and Characterization of Novel Tetradentate Ruthenium Complexes of a Pyridine-*o*-phenylenediamine Based Chelate Ligand

Maryanne K. Stones, Ryan J. Sullivan, Dmitriy V. Soldatov, Marcel Schlaf

PII: S0020-1693(19)31640-8
DOI: https://doi.org/10.1016/j.ica.2019.119391
Reference: ICA 119391

To appear in: *Inorganica Chimica Acta*

Received Date: 27 October 2019
Revised Date: 18 December 2019
Accepted Date: 19 December 2019

Please cite this article as: M.K. Stones, R.J. Sullivan, D.V. Soldatov, M. Schlaf, Synthesis and Characterization of Novel Tetradentate Ruthenium Complexes of a Pyridine-*o*-phenylenediamine Based Chelate Ligand, *Inorganica Chimica Acta* (2019), doi: https://doi.org/10.1016/j.ica.2019.119391

Synthesis and Characterization of Novel Tetradentate Ruthenium Complexes of a Pyridine-*o*-phenylenediamine Based Chelate Ligand.

Maryanne K. Stones, Ryan J. Sullivan, Dmitriy V. Soldatov, and Marcel Schlaf*

Department of Chemistry, University of Guelph, The Guelph-Waterloo Centre for Graduate Work in Chemistry (GWC)^2, 50 Stone Road East, Guelph, Ontario, Canada, N1G 2W1

*Corresponding author: mschlaf@uoguelph.ca

Highlights

- Tetradentate ligands
- High-temperature stable ruthenium complexes
- Potential Hydrogenation catalysts

Abstract

The synthesis of the new complexes [cis-Ru(N,N'-bis-(2-pyridylmethyl)-*o*-phenylenediamine)(Cl)(DMSO)](Cl), [cis-Ru(N,N'-bis-(2-pyridylmethyl)-*o*-phenylenediamine)$(MeCN)_2](OTf)_2$ and [cis-Ru(N,N'-bis-(2-pyridylmethyl)-*o*-phenylenediamine)$(PhCN)_2](OTf)_2$ is reported. The ligand, N,N'-bis-(2-pyridylmethyl)-*o*-phenylenediamine, was complexed to ruthenium using the ruthenium precursor, $RuCl_2(DMSO)_4$, to yield the intermediate complex [cis-Ru(N,N'-bis-(2-pyridylmethyl)-*o*-phenylenediamine)(Cl)(DMSO)](Cl). The metathesis of DMSO and chloride ligands from [cis-Ru(N,N'-bis-(2-pyridylmethyl)-*o*-phenylenediamine)(Cl)(DMSO)](Cl) was carried out in the appropriate nitrile solvent with 2 equivalents of AgOTf to yield the complexes [cis-Ru(N,N'-bis-(2-pyridylmethyl)-*o*-phenylenediamine)$(MeCN)_2](OTf)_2$ and [cis-Ru(N,N'-bis-(2-pyridylmethyl)-*o*-phenylenediamine)$(PhCN)_2](OTf)_2$. Both complexes were characterized by single crystal XRD. [cis-Ru(N,N'-bis-(2-pyridylmethyl)-*o*-phenylenediamine)$(MeCN)_2](OTf)_2$ and [cis-Ru(N,N'-bis-(2-pyridylmethyl)-*o*-phenylenediamine)$(PhCN)_2](OTf)_2$ both possess the hypothetical characteristics of homogeneous hydrogenation catalysts that are anticipated to be acid- water- and temperature stable, and have the potential to be tested as such.

Introduction

In recent years there has been significant effort directed towards the development of efficient catalytic systems to transform and valorize biomass-derived substrates – and even biomass directly – to compete with fossil-based carbon sources for the petrochemical industry [1]. This field has typically been dominated by heterogeneous catalysts [2-7] due to their relative ease of industrial application. However, biomass-derived substrates pose interesting challenges in heterogeneously catalyzed conversions such as coking, fouling and – in consequence – deactivation of the solid catalysts through humin formation which is brought about by the high intrinsic self-reactivity of the sugar substrates [8-10]. An alternative approach is the design and synthesis of molecularly well-defined homogeneous catalytic systems that in principle can effect the same desired transformations [11-13].

While homogeneous catalysts can in specific cases offer advantages over heterogeneous catalysts in the field of biomass conversion, and catalysis generally, there also exist significant barriers and challenges to their success; notably their temperature stability and recyclability. Through iterative design and testing, we have, over the past 15 years [14-17], proposed several generations of homogeneous ruthenium-based catalysts employing chelating pyridine-motif ligands with increasing water, acid, and temperature stability. In addition, the research groups of Leitner, Miller, as well as ourselves, have explored the use of Ru-triphos-based catalyst systems for the hydrodeoxygenation of biomass derived substrates [18-20]. Despite substantial progress, an acid, water- and high-temperature stable, recyclable and promiscuous homogeneous hydrodeoxygenation catalyst has however yet to be discovered.

The work described herein describes a further iteration of homogeneous ruthenium-based catalyst design which was proposed based on the following principles [11]:

(1) The pairing of a cationic complex with non-coordinating counterions such as triflate, should impart solubility in polar reaction media, i.e., ideally pure water;

(2) Based on the chelate effect as the guiding design principle, the increase in ligand denticity from di- and tri- to tetra-dentate will increase the complex formation constant and ultimately impart greater complex stability at the elevated temperatures (150 °C or greater) required for acid-catalyzed dehydration of the substrates; [21]

(3) The metal-ligand system must present at least one labile ligand which, upon dissociation, will render it capable of the heterolytic activation of dihydrogen to perform ionic hydrogenation and/or hydrogenolysis reactions; [22, 23]

(4) Incorporation of an N-H function into the ligand backbone provides the potential for a metal-ligand bifunctional hydrogenation and/or hydrogenolysis mechanism.

To this end, two novel tetradentate, ruthenium centered complexes employing the known ligand N,N'-bis-(2-pyridylmethyl)-*o*-phenylenediamine (**1**) were synthesized and characterized by single crystal X-ray diffraction, mass spectrometry and NMR.

Scheme 1 shows the synthetic pathway to the two complexes.

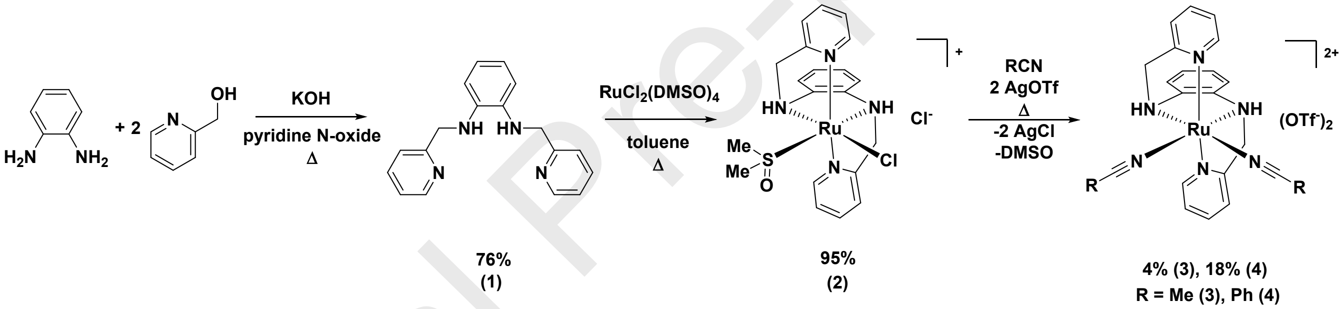

Scheme 1. Synthetic Pathway to [*cis*-Ru(N,N'-bis-(2-pyridylmethyl)-*o*-phenylenediamine)(MeCN)$_2$](OTf)$_2$ (**3**) and [*cis*-Ru(N,N'-bis-(2-pyridylmethyl)-*o*-phenylenediamine)(PhCN)$_2$](OTf)$_2$ (**4**).

To our knowledge, these are the first examples of metal coordination to **1**, however, there exist several previous examples of metal coordination to analogues of **1** that are displayed in Scheme 2. It shows the only example of coordination of **5** [24] to an iron centre. There are many literature examples of **6** [25] coordinating to various metal centres (here shown with a Mn centre as an example) in the presence of secondary ligands. It is interesting to note that in some examples of metal coordination to analogues of **1**, the coordination environment is *cis*, whereas in other examples a *trans* coordination environment is observed. Florián *et al.* [26] studied the geometric isomerization of **7** between *cis* and *trans* coordination environments, which is possible due to the flexibility of this hexadentate ligand. The only other example of **7** reported in the literature features a lanthanum centre (La^{3+}) in place of gallium.

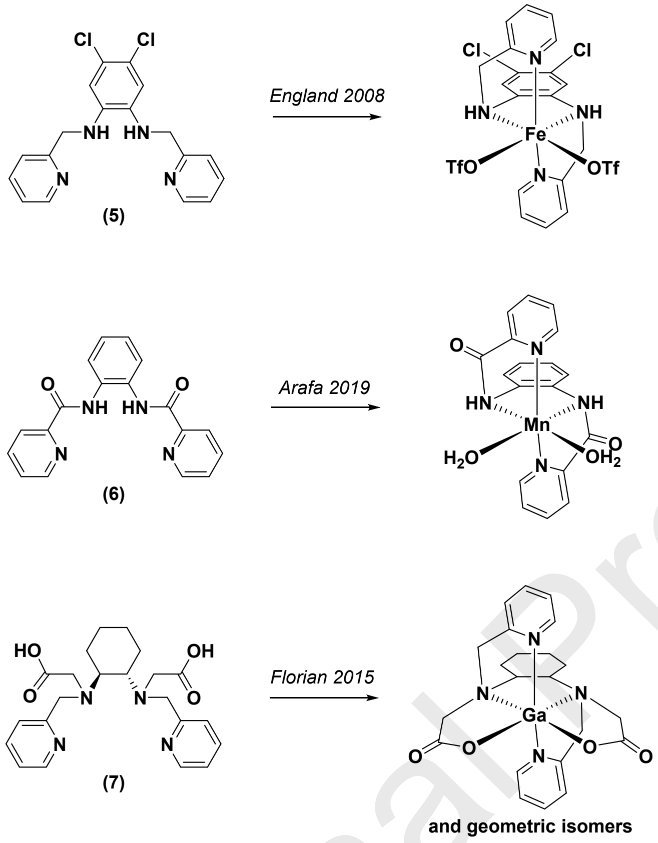

Scheme 2. Literature examples of metal coordination to analogues of **1**. [24-26]

Results and Discussion

Ligand **1** was chosen due to the potentially tetradentate binding pocket provided by four nitrogen atoms, thus increasing the electron density of the metal centre. The phenylene backbone of **1** was hypothesized to impart rigidity in the ligand and thus postulated to increase the binding energy to a metal centre. The positively polarized hydrogens bound to the amine nitrogens are anticipated to act as proton donors in a conceivable ruthenium-hydride/amine mediated metal-ligand bifunctional mechanism, as, e.g., described by Crabtree [27], Noyori [28], Ikariya [29], Morris [30], and Gordon [31], as well by ourselves, uniquely under aqueous acidic conditions [32].

The synthesis of **1** was carried out according to literature procedures outlined by Miyano *et al.* [33, 34] as already described in Scheme 1 above. Purification of **1** as described in literature – by vacuum distillation – proved to be difficult as a tacky, viscous, orange liquid was obtained unlike the solid described in literature. The product would cool to a viscous, honey-like material inside of the distillation apparatus, and constant heating of the entire apparatus using a heat gun was required to pass the entirety the material through to the receiving flask. Notably, England *et al.* [24] also describe a lack of reproducibility with the original procedure [33, 34] as they only obtained starting material and no bis(pyridylmethyl) diamine product.

Despite difficulties with product purification, the ^{1}H and ^{13}C NMR spectra of **1** are well defined and show pure product. (cf. images of spectra supplied in the Supplementary Material). Coordination reactions of the ligand with ruthenium were therefore successfully carried out with the viscous liquid product obtained.

1 was reacted with $RuCl_2(DMSO)_4$ [35], in 1:1 stoichiometry as a suspension in toluene. This reaction produced [*cis*-Ru(N,N'-bis-(2-pyridylmethyl)-*o*-phenylenediamine)(Cl)(DMSO)](Cl) (**2**) in nearly quantitative yield as a dark yellow/brown powder. The identity of **2** was confirmed by ^{1}H, and ^{13}C NMR as well as MS (cf. Supplementary Material). Although in Scheme 1, **2** has been drawn with a sulfur coordinated DMSO ligand – postulated based on the assumption that the oxygen coordinated DMSO would be much more labile than the sulfur coordinated version [35] – it is also possible that the DMSO ligand is instead oxygen coordinated, or a mixture of both is present.

When **2** was initially synthesized, a *trans* coordination motif was anticipated, but the NMR spectra provided direct evidence towards a *cis* coordination. In a *trans* coordination, only 8 individual signals of the **1** backbone would be present due to the compound symmetry, but instead these signals are split due to the asymmetric environment induced by the *cis* coordination motif. **2** was found to be air stable for short periods of time, but the colour of the complex will gradually darken from yellow to brown upon exposure to air indicating decomposition.

Because of the strong binding properties of chloride and DMSO (and its potential products under reducing conditions, e.g., dimethyl sulfide) **2** is not suitable as a catalyst for heterolytic hydrogen activation, which requires the irreversible generation of free coordination sites generated through loss of labile spectator ligands that cannot impede catalysis by coordinative inhibition. Therefore complex **3** was synthesized from **2** via a metathesis reaction of the chloride ligands bound to ruthenium by silver triflate in acetonitrile at elevated temperatures. The concomitant removal of the DMSO ligand required elevated temperatures, well above the boiling point of acetonitrile. Therefore, the reaction was carried out at 175 °C in a pressure sealed 316SS Autoclave Engineers mini-reactor. This reaction yielded **3** as a light brown powder, however only in a 4 % yield following isolation and purification. It is likely that the low yields are a result of both product loss during purification, and incomplete conversion to product. Because the DMSO ligand cannot be scavenged by silver ions, even if it dissociates from the ruthenium centre, it binds much more strongly to the ruthenium centre than the labile acetonitrile ligands and could re-coordinate. While the yield of this process is very low, the ability of **3** to survive temperatures of 175 °C shows promise for **1** as a ligand in biomass conversion chemistry which requires temperatures of >150 °C.

Despite low product yields, a crystal suitable for single crystal X-ray analysis could be obtained by vapour diffusion of diethyl ether into a saturated product solution of methylene chloride. The identity of **3** was confirmed by ^{1}H NMR, ^{13}C NMR, MS and single crystal XRD (cf. Supplementary Material for images of spectra and references to crystal data/CIF in the CCDC) [36]. Figure 1 shows an ORTEP and the asymmetric unit cell of **3**, which displayed disorder in two of the triflate counterions. The crystal structure confirms the cis coordination environment of **1** complexed to the ruthenium centre, which is expected from **2** also displaying a cis coordination environment.

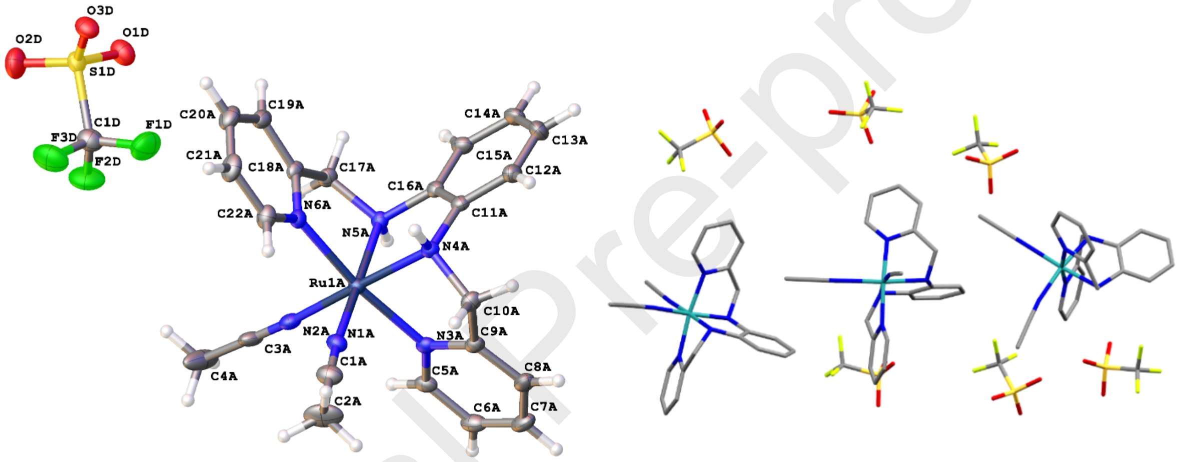

Figure 1: ORTEP and capped stick rendering of the asymmetric unit cell of **3** (hydrogens and disorder of the triflate counterions omitted for clarity in the right image).

The low yields of **3** obtained – and the inability to scale up the reaction inside of a limited volume pressure vessel – prompted a switch in reaction solvent from acetonitrile to the much higher boiling benzonitrile. The synthesis of **4** was again carried out with silver triflate being used to scavenge the chloride ligand, but could be performed at ambient pressure at 200 °C. This reaction yielded **4** in an 18 % yield as a pink/red powder, a significant improvement from the reaction carried out in acetonitrile to yield **3**. It is conceivable that the increased temperature of the reaction promoted a greater dissociation of the DMSO ligand, resulting in an increased yield. The ambient pressure reaction is also more convenient for scale-up as it can be carried out in the appropriate benchtop glassware and should be amenable to further optimization as a function of reaction temperature, time, and volume, which was however beyond the scope of this initial study.

As with **3** crystals suitable for single crystal X-ray analysis were grown by vapour diffusion of diethyl ether into a saturated product solution of methylene chloride. The identity of **4** was confirmed by ^{1}H and ^{13}C NMR, IR, MS, and single crystal XRD. Figure 2 shows an ORTEP and the asymmetric unit cell of **4** which, unlike the asymmetric unit cell of **3**, only contains one metal coordinated complex instead of three. **4** also contains a water molecule, which may have either aided in the crystallization process or been trapped inside the crystal lattice. As Figure 2 illustrates, **4** was also confirmed to exist as a *cis* coordination environment.

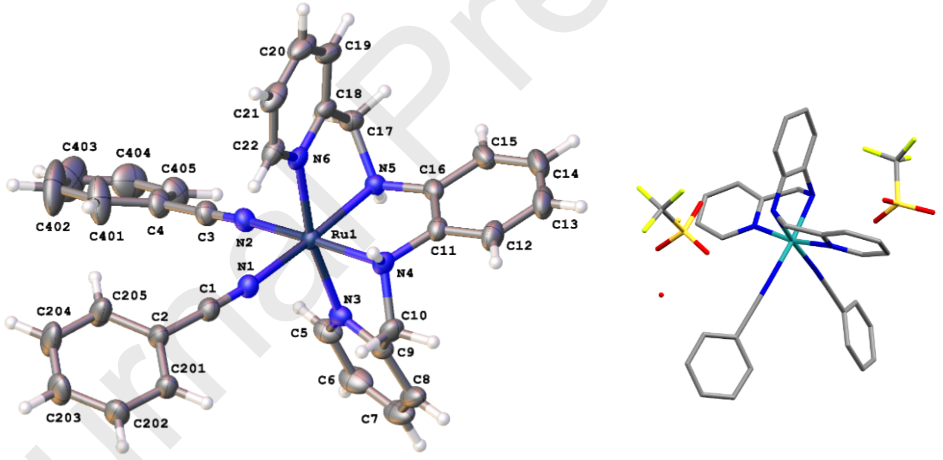

Figure 2: ORTEP and capped stick rendering of the asymmetric unit cell of **4** (hydrogens omitted for clarity).

Table 1 lists and compares the bond distances and angles of the ruthenium coordination environment in **3** and **4**. The bond distances fall in the expected ranges for Ru^{II}-N bonds with neutral ligands (~ 2 Å). The bond angles in the planar chelate (N5-Ru-N4) are ~ 83.7 ° and 79.5-81° for the non-planar (N3-Ru-N4 and N6-Ru-N5) 5-membered chelate rings. The former fall in the middle of the range (81.3° and 86.0°) for the only other dicationic ruthenium complexes reported in the CCDC 2019 database (deposition numbers 1565148 and 1565149) that pair a neutral phenylene-diamine with pyridine ligands [37].

Table 1: Bond length and angles of the Ruthenium coordination environment in **3** and **4**.[a]

Bond Length [Å]	**3** (R = CH_3CN)[b]	**4** (R = PhCN)
Ru-N1	2.021(3)	2.0075(16)
Ru-N2	2.029(3)	2.0138(17)
Ru-N3	2.082(3)	2.0658(16)
Ru-N4	2.087(3)	2.0887(16)
Ru-N5	2.082(3)	2.0847(15)
Ru-N6	2.063(3)	2.0735(16)
Bond Angles [°]		
N1-Ru1-N2	91.65(14)	87.55(7)
N1-Ru1-N6	95.37(13)	95.17(7)
N2-Ru1-N6	88.95(12)	93.27(6)
N1-Ru1-N3	88.75(13)	92.87(6)
N2-Ru1-N3	97.65(13)	94.38(7)
N6-Ru1-N3	172.14(13)	169.13(6)
N1-Ru1-N5	173.76(13)	174.78(6)
N2-Ru1-N5	93.33(13)	94.21(6)
N6-Ru1-N5	80.97(12)	79.83(6)
N3-Ru1-N5	94.31(12)	91.90(6)
N1-Ru1-N4	91.89(13)	95.00(6)
N2-Ru1-N4	175.39(13)	174.64(7)
N6-Ru1-N4	93.67(12)	91.19(6)
N3-Ru1-N4	79.48(12)	80.80(7)
N5-Ru1-N4	83.34(12)	91.19(6)

[a]Complete tables of all structural and data collection parameters for **3** and **4** can be found in the Supplementary Material and in the CIF files deposited with the CCDC (**3:** #1961063; **4:** #1961064). [b]Atoms for **3** labeled as A in the ORTEP in Figure 1 by selection of one of the three cations in the asymmetric unit cell.

An alternative to the use of monodentate nitrile solvents in the metathesis step, would the use of bidentate nitrile solvents such as succinonitrile or glutaronitrile. The chloride metathesis is driven by the precipitation of silver chloride and will yield a free coordination site for coordination of one nitrogen of the bidentate ligand to coordinate. This could more easily drive the dissociation of the DMSO ligand due to the formation of a secondary chelate ligand. Further experiments using this approach should result in optimization of the yields of analogues of **3** and **4** allowing for them to be tested as catalysts for the hydrodeoxygenation of biomass-derived, substrates in aqueous-acidic media at temperatures at least equivalent to that of the boiling point of benzonitrile (191 °C).

Experimental section

General All reagents and solvents were purchased from readily available commercial sources and used as received unless otherwise specified. The neutral Al_2O_3 used for column chromatography had a Brockmann Activity I. Manipulations performed under inert atmospheric conditions were carried out using degassed solvents and standard Schlenk vacuum line techniques under an inert argon atmosphere. All NMR spectra were gathered on a 400 MHz spectrometer and calibrated to the residual solvent shift. Single crystal X-ray diffraction analysis were carried out on an Agilent SuperNova Single Crystal X-Ray Diffractometer. Mass spectral data were collected on a Bruker AmaZon SL LC-MS^n bypassing the LC and instead using direct injection with electrospray ionization (ESI).

N,N'-bis-(2-pyridylmethyl)-*o*-phenylenediamine (1). o-phenylenediamine (3.2033 g, 29.62 mmol), 2-pyridinemethanol (7.7447 g, 70.97 mmol), pyridine 1-oxide (0.0295 g, 0.31 mmol) and KOH (0.6880 g, 12.26 mmol) were combined in a round bottom flask with still head apparatus. Incremental heating of the flask to 225 ºC resulted in a vigorous boiling reaction with yellow solid forming in the flask. 1.6 mL of distillate was collected at a vapour temperature of 100 ºC. The flask was cooled to room temperature. H_2O (25 mL) was added and neutralized with HCl to pH 7. The product was extracted with $CHCl_3$ (2 x 25 mL) and the remaining solvent removed under vacuum. A fractional distillation was performed on crude product with yellow oil distilling off at 170 ºC, 160 mTorr. Two fractions were collected. Fraction 1 yield: 3.1294 g, 36%. Fraction 2 yield: 2.1688 g, 25%. The first fraction was purified by silica packed column chromatography (30 x 300 mm) with a 20:1 acetonitrile:methanol mobile phase. Two distinct yellow bands passed through the column, the latter being the product. The product was collected, and solvent removed under vacuum. Column fraction yield: 1.2903 g, 15%. Total yield: 3.4618 g, 40%. ^{1}H NMR (400

MHz, $CDCl_3$): δ= 4.46 (s, 6H), 6.66 (m, 2H), 6.75 (m, 2H), 7.18 (tdd, J_1=6.16 Hz, J_2=1.12 Hz, J_3=1.12 Hz, 2H), 7.36 (d, J=7.84 Hz, 2H), 7.64 (td, J_1=7.74 Hz, J_2=1.81 Hz, 2H), 8.59 (dq, J_1=4.87 Hz, J_2=0.88 Hz, 2H). ^{13}C NMR (400 MHz, $CDCl_3$): δ= 49.9 (CH_2), 112.2 (CH), 119.4 (CH), 121.7 (CH), 122.1 (CH), 136.6 (CH), 137.0 (C), 149.3 (CH), 158.9 (C).

$RuCl_2(DMSO)_4$.[35] $RuCl_3 \cdot xH_2O$ (2.0348 g, 7.78 mmol) was dissolved in ethanol (50 mL) and brought to reflux at 100 ºC with stirring. The solution was refluxed for 4 h and then cooled to room temperature. The dark green solution was filtered, and the solvent evaporated, leaving a dark green oil. DMSO (8 mL) was added and the solution submerged in an oil bath pre-heated to 150 ºC, resulting in a colour change to bright orange with yellow precipitate. The solution was refluxed for 2 h then cooled to room temperature. Acetone (60 mL) was added to complete precipitation and the suspension was left to settle overnight. The bright yellow product was collected by vacuum filtration, washing with acetone. Crude yield: 2.8809 g, 76 %. The product was then recrystallized from a minimal amount of hot DMSO and collected by vacuum filtration, washing with acetone. The bright yellow crystals were then dried under vacuum. Yield: 2.3871 g, 63 %.

[*cis*-Ru(N,N'-bis-(2-pyridylmethyl)-*o*-phenylenediamine)(Cl)(DMSO)](Cl) (2). This reaction was carried out using standard Schlenk techniques. Toluene (100 mL) was added to a flask containing N,N'-bis-(2-pyridylmethyl)-*o*-phenylenediamine (638.2 mg, 2.20 mmol) and $RuCl_2(DMSO)_4$ (1.0719 g, 2.21 mmol). The yellow suspension was heated to reflux with stirring. The solution was refluxed at 125 ºC for 20 h. The yellow powder was then vacuum filtered via Buchner funnel, washing with the mother liquor three times. The product was collected and dried under vacuum. Yield: 1.1352 g, 95%. ^{1}H NMR (400 MHz, CD_3CN): δ = 4.50 (d, J=16.24 Hz, 1H), 4.63 (d, J=15.28 Hz, 1H), 4.90 (dd, J_1=16.28 Hz, J_2=5.4 Hz, 1H), 5.51 (dd, J_1=15.16 Hz, J_2=4.88 Hz, 1H), 6.83 (d, J=4.84 Hz, 1H), 7.31 (m, 5H), 7.40 (t, J=6.68 Hz, 1H), 7.50 (dd, J_1=7.84 Hz,

J_2=1.44 Hz, 1H), 7.63 (m, 2H), 7.75 (m, 2H), 9.20 (dd, J_1=6.2 Hz, J_2=1.52 Hz, 1H), 9.33 (dd, J_1=5.68 Hz, J_2=0.84 Hz, 1H). ^{13}C NMR (400 MHz, CD_3CN): δ = 61.4 (CH_2), 64.5 (CH_2), 122.3 (CH), 122.5 (CH), 124.0 (CH), 124.3 (CH), 126.4 (CH), 126.9 (CH), 129.1 (CH), 129.4 (CH), 136.8 (CH), 137.3 (CH), 143.4 (C), 145.1 (C), 153.6 (CH), 156.2 (CH), 161.2 (C), 161.9 (C). *m/z* 504.99 [$C_{20}H_{24}ClN_4ORuS$]$^+$.

[Ru(N,N'-bis-(2-pyridylmethyl)-*o*-phenylenediamine)(MeCN)$_2$](OTf)$_2$ (3). Acetonitrile (35 mL) was added to a flask containing [cis-Ru(N,N'-bis-(2-pyridylmethyl)-*o*-phenylenediamine)(Cl)(DMSO](Cl) (296.6 mg, 0.55 mmol) and AgOTf (297.7 mg, 1.16 mmol). The resulting solution was green with a brown suspension. The solution was heated to 175 ºC with stirring in an Engineers Autoclave mini-reactor for 20 h. The solution was cooled to room temperature and vacuum filtered through a frit with Celite® to remove the grey AgCl precipitate. The resulting bright red solution was evaporated and dried under vacuum resulting in a bright red oil. Crude yield: 546.4 mg, 86 %. The crude product was then purified on a neutral alumina column (30 x 330 mm) with a 2:1 acetonitrile:toluene mobile phase and the yellow/brown band was collected. The solvent was removed by rotary evaporation and the dark orange oil was dried under vacuum. The sample was dissolved in acetonitrile (6 mL) and precipitated with diethyl ether (60 mL) resulting in a light brown powder which was collected on a frit and dried under vacuum. Yield: 14.9 mg, 4 %. Crystals suitable for single crystal X-ray diffraction analysis were grown by vapour diffusion of diethyl ether into a saturated solution of methylene chloride. ^{1}H NMR (400 MHz, CD_3CN): δ= 4.61 (d, J=16.11 Hz, 2H), 4.87 (dd, J_1=16.04 Hz, J_2=5.28 Hz, 2H), 7.11 (d, J=4.96 Hz, 2H), 7.36 (m, 6H), 7.52 (q, J=3.44 Hz, 2H), 7.73 (td, J_1=7.74 Hz, J_2=1.48 Hz, 2H), 9.012 (d, J=5.08 Hz, 2H). ^{13}C NMR (400MHz, CD_3CN): δ= 63.3 (CH_2), 122.9 (CH), 124.8 (CH), 126.9 (CH), 130.4 (CH), 138.0 (CH), 144.9 (C), 154.8 (CH), 161.4 (C). *m/z*: 623.01 [$C_{23}H_{24}F_3N_6O_3RuS$]$^+$.

[Ru(N,N'-bis-(2-pyridylmethyl)-*o*-phenylenediamine)(PhCN)$_2$](OTf)$_2$ (4). Benzonitrile (20 mL) was added to [Ru(N,N'-bis-(2-pyridylmethyl)-*o*-phenylenediamine)(Cl)(DMSO)](Cl) (101.9 mg, 0.19 mmol) and AgOTf (100.3 mg, 0.39 mmol) and the solution was brought to reflux at 200 °C with stirring for 16 h. The solution was then filtered through a frit with Celite® to remove the grey AgCl, resulting in a dark red solution. The solvent was distilled off *in vacuo*, leaving a dark red oil. The crude product was purified on a neutral alumina column (20 x 200 mm) with a 2:1 acetonitrile:toluene mobile phase and the red band was collected. The solvent was removed by rotary evaporation. The red solid was dissolved in a minimal amount of acetonitrile and precipitated with diethyl ether yielding a pink/red powder which was collected on a frit and dried under vacuum. Yield: 19.9 mg, 18 %. Crystals suitable for single crystal X-ray diffraction analysis were grown by vapour diffusion of diethyl ether into a saturated solution of methylene chloride. ^{1}H NMR (400 MHz, CD_2Cl_2): δ= 4.63 (2H, d, J=16.4 Hz), 5.21 (2H, dd, J = 5.6, 16 Hz), 7.26 (2H, d, J = 7.6 Hz), 7.31 (2H, dd, J = 2.4, 3.6 Hz), 7.37 (2H, t, J = 5.6 Hz), 7.56 (4H, t, J = 8 Hz), 7.65 (6H, m), 7.98 (4H, dd, J = 8.4, 0.1 Hz), 9.18 (2H, d, J = 4.8). ^{13}C NMR (400 MHz, CD_2Cl_2): δ= 64.1 (CH_2), 111.9 (C), 122.3 (CH), 124.7 (CH), 126.4 (CH), 127.3 (C), 129.7 (CH), 130.1 (CH), 133.9 (CH), 134.1 (CH), 144.6 (C), 154.7 (CH), 160.8 (C). ATR-IR (solid, cm^{-1}): 3096w, 3066w, 1596w, 1489s, 1447s, 1262s, 1222s, 1140s, 1029s, 1000w, 934w, 753s, 683s, 635s, 572s, 552s, 515s. *m/z*: 747.07 $[C_{33}H_{28}F_3N_6O_3RuS]^+$.

Supplementary Material: Details of synthetic procedures, spectral data and images of ^{1}H/^{13}C NMR spectra, Tables of crystallographic data and ORTEPs (pdf file 75 pages). CIF files have been deposited with and are available from the Cambridge Crystallographic Data Centre. CCDC codes: **3** #1961063; **4** #1961064. The data can be obtained free of charge from The Cambridge Crystallographic Data Centre via www.ccdc.cam.ac.uk/structures.

Acknowledgment: This work was supported by the Discovery Grant Program of the Natural Science and Engineering Research Council of Canada (NSERC) and the Bioeconomy Program of the Ontario Ministry of Agriculture, Food and Rural Affairs (OMAFRA).

Literature References

[1] R.A. Sheldon, Green Chem., 16 (2014) 950-963.
[2] J.N. Chheda, J.A. Dumesic, Catal. Today, 123 (2007) 59-70.
[3] A. Corma, S. Iborra, A. Velty, Chem. Rev., 107 (2007) 2411-2502.
[4] D.M. Alonso, S.G. Wettstein, J.A. Dumesic, Chem. Soc. Rev., 41 (2012) 8075-8098.
[5] M.J. Climent, A. Corma, S. Iborra, Green Chem., 16 (2014) 516-547.
[6] D.L. Sun, S. Sato, W. Ueda, A. Primo, H. Garcia, A. Corma, Green Chem., 18 (2016) 2579-2597.
[7] W.H. Luo, W.X. Cao, P.C.A. Bruijnincx, L. Lin, A.Q. Wang, T. Zhang, Green Chem., 21 (2019) 3744-3768.
[8] I. van Zandvoort, Y.H. Wang, C.B. Rasrendra, E.R.H. van Eck, P.C.A. Bruijnincx, H.J. Heeres, B.M. Weckhuysen, ChemSusChem, 6 (2013) 1745-1758.
[9] Z.W. Cheng, J.L. Everhart, G. Tsilomelekis, V. Nikolakis, B. Saha, D.G. Vlachos, Green Chem., 20 (2018) 997-1006.
[10] H.F. Xiong, H.N. Pham, A.K. Datye, Green Chem., 16 (2014) 4627-4643.
[11] M. Schlaf, Dalton Trans., (2006) 4645-4653.
[12] P.J. Deuss, K. Barta, J.G. de Vries, Catal. Sci. Technol., 4 (2014) 1174-1196.
[13] M. Schlaf, Homogeneous Catalysts for the Hydrodeoxygenation of Biomass Derived Carbohydrate Feedstocks, in: M. Schlaf, Z. Zhang (Eds.) Reaction Pathways and Mechanisms in Thermocatalytic Biomass Conversion - Green Chemistry and Sustainable Technology Series, Springer Beijing, Vol 2., (2015), 13-38.
[14] R.R. Dykeman, K.L. Luska, M.E. Thibault, M.D. Jones, M. Schlaf, M. Khanfar, N.J. Taylor, J.F. Britten, L. Harrington, J. Mol. Catal. A-Chem., 277 (2007) 233-251.
[15] M.E. Thibault, D.V. DiMondo, M. Jennings, P.V. Abdelnur, M.N. Eberlin, M. Schlaf, Green Chem., 13 (2011) 357-366.
[16] Z. Xie, M. Schlaf, J. Mol. Catal. A-Chem., 229 (2005) 151-158.
[17] D. Taher, M.E. Thibault, D. Di Mondo, M. Jennings, M. Schlaf, Chem.-Eur. J., 15 (2009) 10132-10143.
[18] E. Latifi, A.D. Marchese, M.C.W. Hulls, D.V. Soldatov, M. Schlaf, Green Chem., 19 (2017) 4666-4679.
[19] F.M.A. Geilen, B. Engendahl, A. Harwardt, W. Marquardt, J. Klankermayer, W. Leitner, Angew. Chem.-Int. Edit., 49 (2010) 5510-5514.
[20] A. Phanopoulos, A.J.P. White, N.J. Long, P.W. Miller, ACS Catal., 5 (2015) 2500-2512.
[21] R.D. Hancock, Chem. Soc. Rev., 42 (2013) 1500-1524.
[22] G. Kubas, Kluwer Academic/ Plenum Publishers: New York, (2001).
[23] R.M. Bullock, Chem.-Eur. J., 10 (2004) 2366-2374.
[24] J. England, C.R. Davies, M. Banaru, A.J.P. White, G.J.P. Britovsek, Adv. Synth. Catal., 350 (2008) 883-897.

[25] W.A.A. Arafa, J. Heterocycl. Chem., 56 (2019) 1403-1412.
[26] J. Florian, C.C. McLauchlan, D.S. Kissel, C.C. Eichman, A.W. Herlinger, Inorg. Chem., 54 (2015) 10361-10370.
[27] D.H. Lee, B.P. Patel, E. Clot, O. Eisenstein, R.H. Crabtree, Chem. Commun., (1999) 297-298.
[28] M. Yamakawa, H. Ito, R. Noyori, J. Am. Chem. Soc., 122 (2000) 1466-1478.
[29] T. Ikariya, Bull. Chem. Soc. Jpn., 84 (2011) 1-16.
[30] S.E. Clapham, A. Hadzovic, R.H. Morris, Coord. Chem. Rev., 248 (2004) 2201-2237.
[31] P.A. Dub, J.C. Gordon, Nat. Rev. Chem., 2 (2018) 396-408.
[32] D. DiMondo, M.E. Thibault, J. Britten, M. Schlaf, Organometallics, 32 (2013) 6541-6554.
[33] S. Miyano, A. Uno, N. Abe, Chem. Pharm. Bull., 15 (1967) 515-+.
[34] S. Miyano, Chem. Pharm. Bull., 13 (1965) 1135-+.
[35] I. Bratsos, E. Alessio, M.E. Ringenberg, T.B. Rauchfuss, Inorganic syntheses, 35 (2010) 148-152.
[36] Cambridge Crystallographic Data Centre; https://www.ccdc.cam.ac.uk/.
[37] K.S. Al-Rashdi, B.A. Babgi, C. Sahin, N.E. Eltayeb, G.J. Moxey, M.G. Humphrey, A.S. Basaleh, Journal of Molecular Structure, 1158 (2018) 197-204.

CRediT author statement

Maryanne K. Stones: Investigation, Data Curation, Visualization, Writing - Original Draft

Ryan J. Sullivan: Investigation

Dmitriy V. Soldatov: Investigation, Data Curation, Visualization

Marcel Schlaf: Conceptualization, Supervision, Funding acquisition, Writing - Review & Editing

Highlights

- **Tetradentate ligands**
- **High-temperature stable ruthenium complexes**
- **Potential Hydrogenation catalysts**

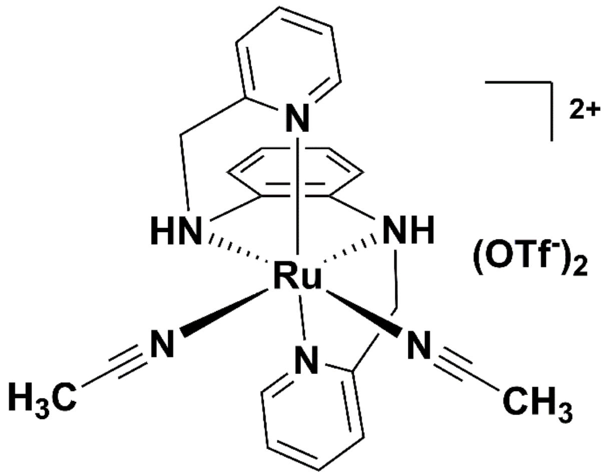
N
HN
NH
Ru
N
N
N
H3C
CH3
2+
(OTf-)2

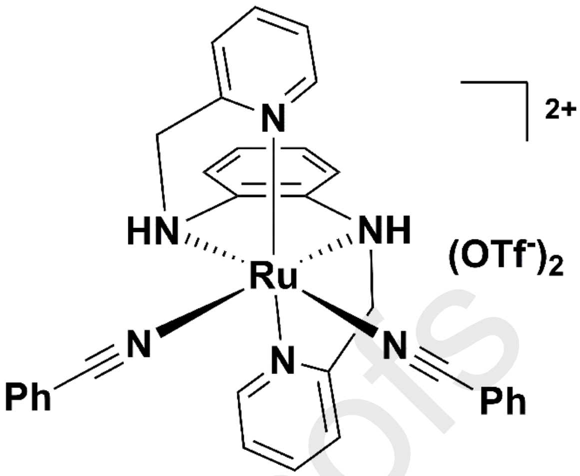
N
HN
NH
Ru
N
N
N
Ph
Ph
2+
(OTf-)2

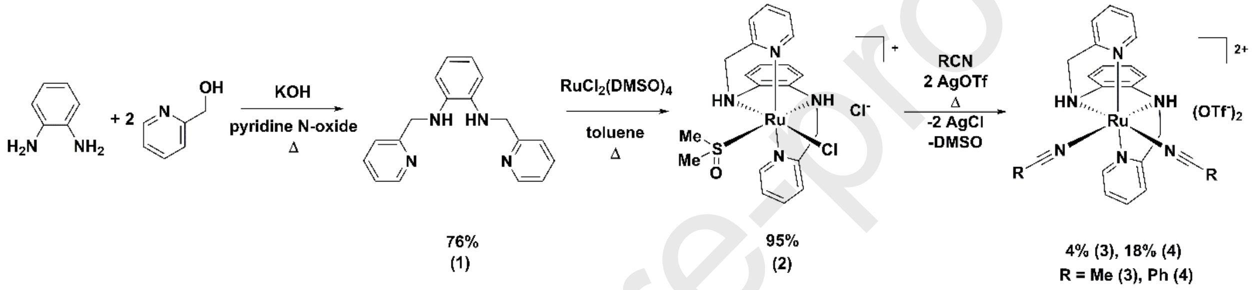
H2N
NH2
+ 2
N
OH
KOH
pyridine N-oxide
Δ
NH
HN
N
N
76%
(1)
RuCl2(DMSO)4
toluene
Δ
HN
NH
Ru
Me
Me
S
O
Cl
Cl-
+
95%
(2)
RCN
2 AgOTf
Δ
-2 AgCl
-DMSO
HN
NH
Ru
R
R
2+
(OTf-)2
4% (3), 18% (4)
R = Me (3), Ph (4)

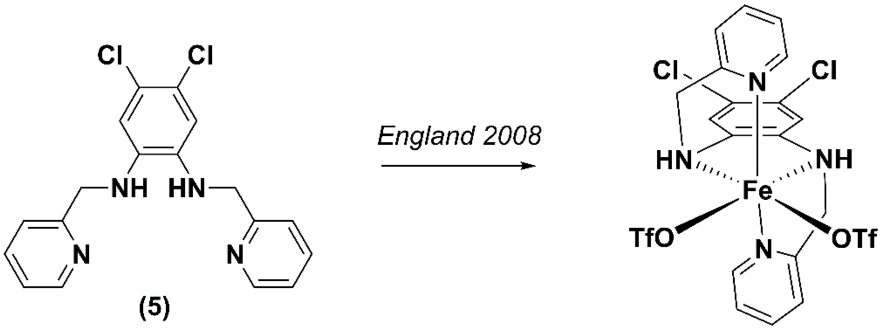

(5)

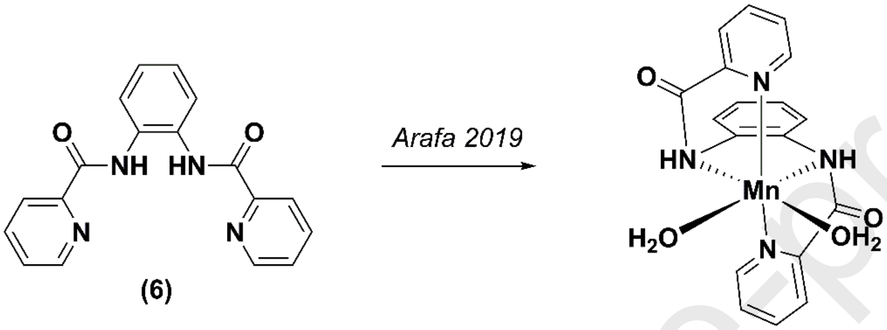

(6)

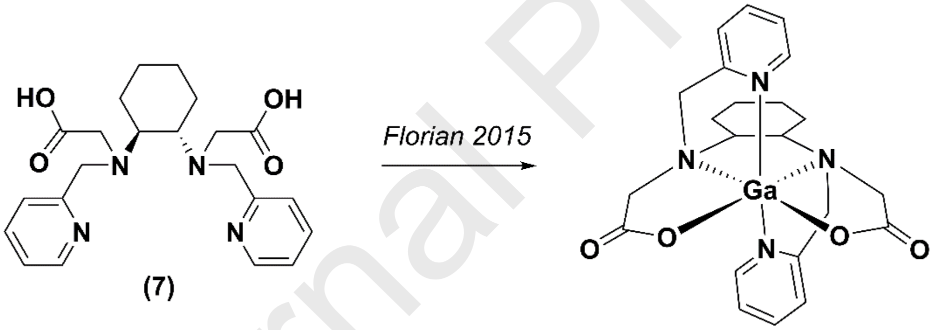

(7)

and geometric isomers

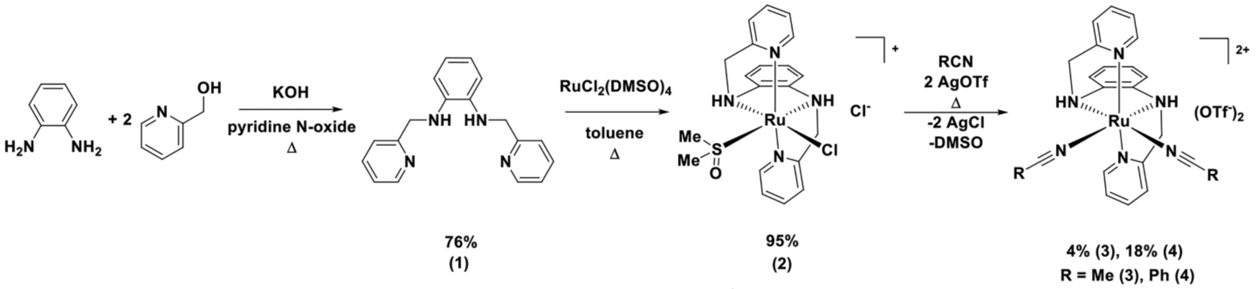

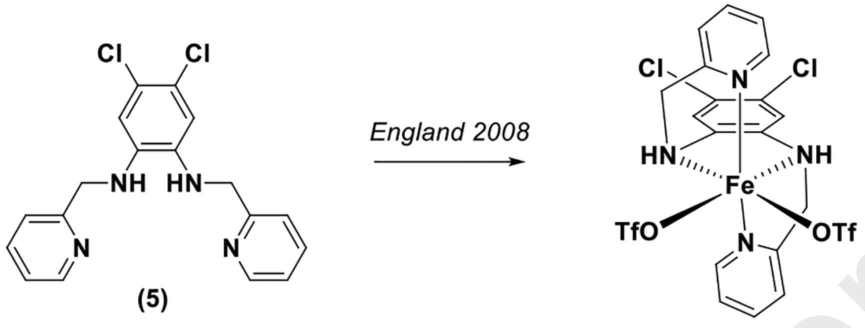

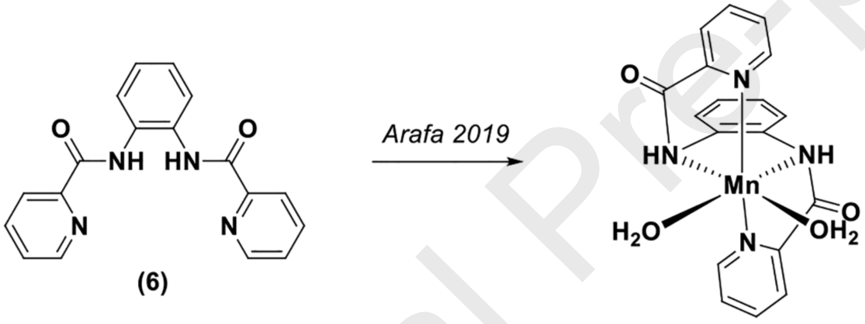

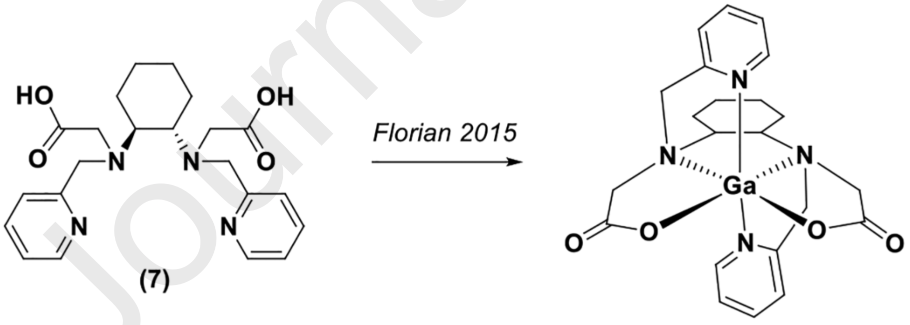

and geometric isomers

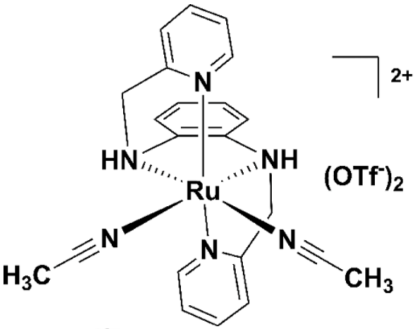
2+
N
HN
NH
Ru
(OTf$^-$)$_2$
N
N
N
H$_3$C
CH$_3$

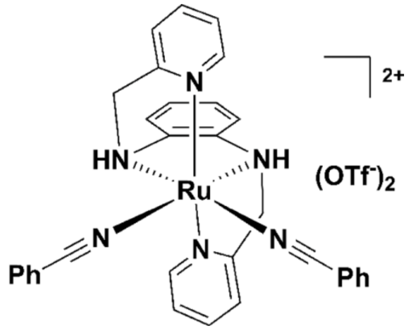
2+
N
HN
NH
Ru
(OTf$^-$)$_2$
N
N
N
Ph
Ph

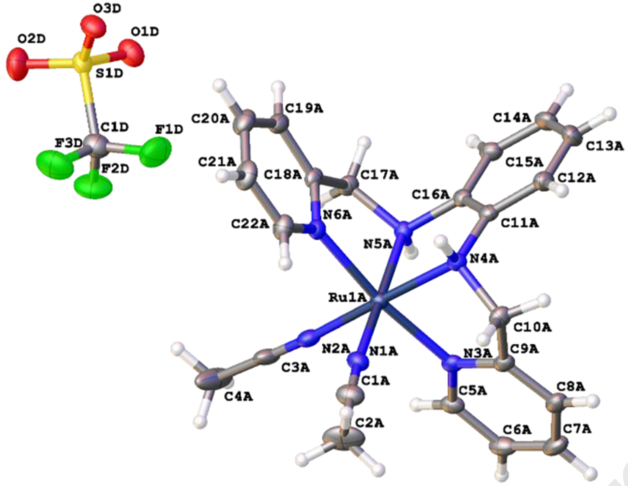
O3D
O2D
O1D
S1D
C1D
F1D
F3D
F2D
C20A
C19A
C21A
C18A
C17A
C14A
C13A
C15A
C12A
C16A
C22A
N6A
N5A
N4A
C11A
Ru1A
C10A
N2A
N1A
N3A
C9A
C3A
C4A
C1A
C5A
C8A
C2A
C6A
C7A

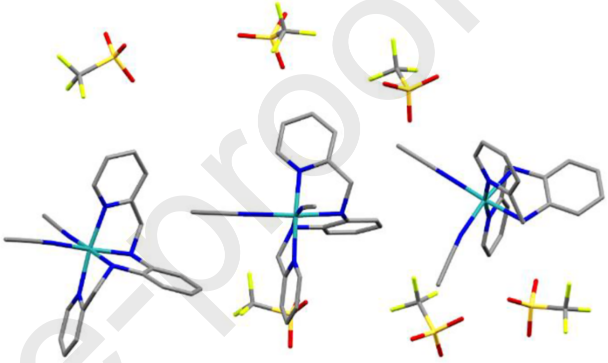

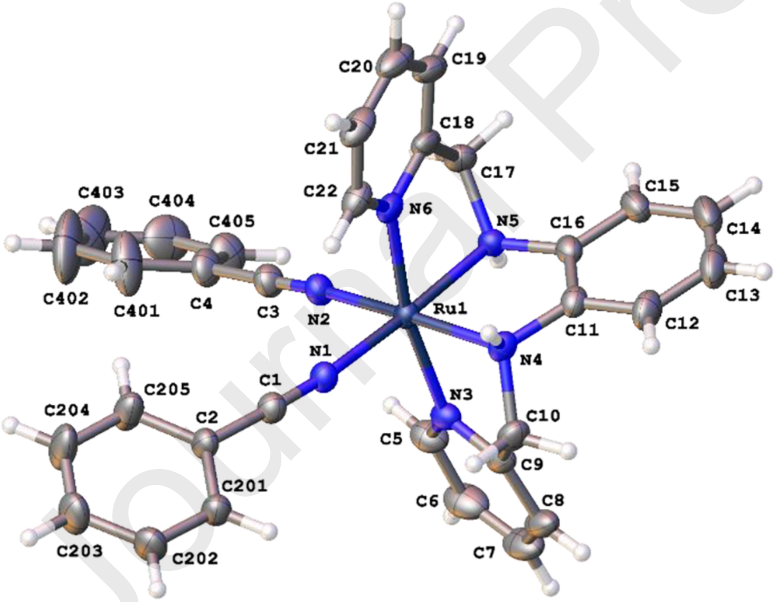
C20
C19
C18
C21
C17
C22
C403
C404
C405
N6
N5
C16
C15
C14
C13
C402
C401
C4
C3
N2
Ru1
C11
C12
N1
N4
C205
C1
C204
C2
N3
C10
C5
C9
C201
C6
C8
C203
C202
C7